Sensor and Simulation Notes

Note 154

July, 1972

Direct Time Domain Analysis of Linear EMP Radiators

by

T. K. Liu
The Dikewood Corporation
Westwood Research Center
Los Angeles, California 90024

Abstract

The space-time integral equation of Hallen's type in describing the transient behavior of linear antennas is derived and solved numerically on a digital computer. This is also applicable in solving problems involving the interaction of EMP and linear wires. With modifications on the formulation and numerical technique, the integral equation is also used to obtain time domain responses of coupled parallel linear antennas, and scatterers with loads, etc.

I. INTRODUCTION

In this note, we present the study of the effect of EMP on linear radiators. The method we use is also useful to the problem of the interaction between EMP and linear wires; this would also be included. Earlier attempts [1] on this transient problem were mainly carried out analytically, transforming frequency formulations into the time domain. The development of fast digital computers with large memory storages has prompted intense computational studies. A commonly used technique in obtaining time domain results is to numerically Fourier transform the computed steady-state solutions. Such a technique was applied to this problem by Tesche [2]. A direct time-domain approach seems to be more appropriate in studying early time behavior, and often offers more physical insight than the steady-state approach. Sayre [3], Bennett and Martine [4] and Miller et al [5] used the time-space integro-differential equations in terms of the electric field. A magnetic field time-space integral equation was used by Bennett and Weeks [6] to treat solid bodies. We here present an alternative approach which results in a Hallen's type integral equation in the time domain, i.e., the space-time derivatives of the equation are eliminated from the integral operator. The solution is carried out numerically on a digital computer.

This method is then extended to treat the problem of coupled parallel wires. In this case, the numerical process is slightly more involved. With some modifications, antennas and scatterers with loads and with losses can readily be solved.

II. MATHEMATICAL FORMULATION

The derivation of the time-domain integral equation proceeds in parallel to that of Hallen's integral equation in the frequency domain.

At a position $\vec{r}$ at time t, the scattered electric field is given by

$$\vec{E}^s(\vec{r},t) = - \nabla\phi(\vec{r},t) - \mu \frac{\partial \vec{A}(\vec{r},t)}{\partial t} , \tag{1}$$

where the vector potential $\vec{A}(\vec{r},t)$ is related to the current density $\vec{J}(\vec{r},t)$ by

$$(\nabla^2 - \mu\varepsilon \frac{\partial^2}{\partial t^2}) \vec{A}(\vec{r},t) = - \vec{J}(\vec{r},t), \tag{2}$$

and the scalar potential $\phi(\vec{r},t)$ is related to $\vec{A}(\vec{r},t)$ by the gauge condition,

$$\nabla\cdot\vec{A}(\vec{r},t) + \varepsilon \frac{\partial\phi(\vec{r},t)}{\partial t} = 0 . \tag{3}$$

The quantities μ and ε are the permeability and the dielectric constant, respectively, of the medium, satisfying the relation $\mu\varepsilon = 1/c^2$, where c is the velocity of light in the medium. The solution of Eq. (2), satisfying the radiation condition at infinity, is,

$$\vec{A}(\vec{r},t) = \iint_S \frac{\vec{J}(\vec{r},t - \frac{|\vec{r}-\vec{r}'|}{c})}{4\pi|\vec{r} - \vec{r}'|} ds', \qquad (4)$$

where s is the surface supporting the source $\vec{J}(\vec{r},t)$.

Specializing Eqs. (1) and (3) to those of a straight wire oriented in the z direction, as shown in Fig. 1, we obtain

$$\frac{\partial A_z(\vec{r},t)}{\partial z} + \varepsilon \frac{\partial \phi(\vec{r},t)}{\partial t} = 0,$$

where $A_z(\vec{r},t)$ is the z component of $\vec{A}(\vec{r},t)$. Using Eq. (1) and the above equation, the z component of the scattered electric field is related to A_z by

$$\varepsilon \frac{\partial E_z^s(\vec{r},t)}{\partial t} = \frac{\partial^2 A_z(\vec{r},t)}{\partial z^2} - \frac{1}{c^2} \frac{\partial^2 A_z(\vec{r},t)}{\partial t^2}. \qquad (5)$$

The total electric field is the sum of the incident electric field and the scattered electric field, and this relation is also true for the z components,

$$E_z(\vec{r},t) = E^{inc}(\vec{r},t) + E_z^s(\vec{r},t) ,$$

where $E^{inc}(\vec{r},t)$ is the z-directed incident electric field. Letting $\vec{r}$ approach the surface of the wire, and using the boundary condition that the total tangential electric field vanishes on the surface of a perfect conductor, we have

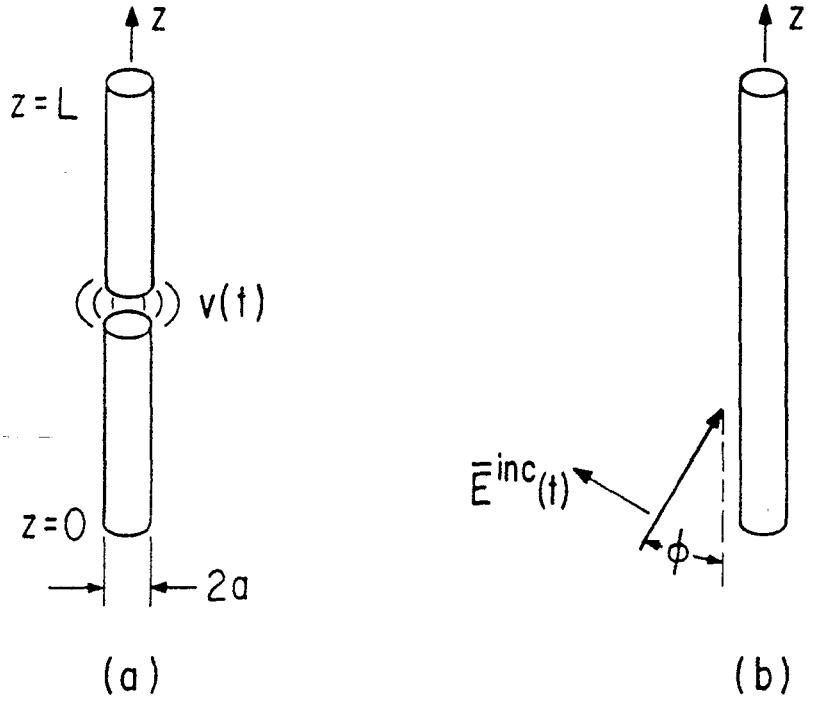

Fig. 1 The configuration of a thin wire as

(a) an antenna, and

(b) a scatterer with $e^{inc}(t)$ at an angle ϕ to the z-axis.

$$\frac{\partial^2 A_z(\vec{r},t)}{\partial z^2} - \frac{1}{c^2}\frac{\partial^2 A_z(\vec{r},t)}{\partial t^2} = -\varepsilon \frac{\partial E^{inc}(\vec{r},t)}{\partial t^2} \quad . \tag{6}$$

A particular solution of Eq. (6) can be obtained by using the new variables,

$$\eta = ct - z,$$

and (7)

$$\xi = ct + z.$$

In terms of ξ, η, Eq. (6) becomes,

$$\frac{\partial^2}{\partial\xi\partial\eta} A_z(\xi,\eta) = \frac{1}{4}\frac{\partial E^{inc}}{\partial t}\left(\frac{\xi-\eta}{2}, \frac{\xi+\eta}{2}\right) \cdot \tag{8}$$

The particular solution of Eq. (8) is,

$$A_z^p(\xi,\eta) = \frac{1}{4}\int_{-\infty}^{\eta}\int_{-\infty}^{\xi} \varepsilon \frac{\partial E^{inc}}{\partial t'}\left(\frac{\xi'-\eta'}{2}, \frac{\xi'+\eta'}{2}\right) d\xi' d\eta' \cdot \tag{9}$$

Changing the variables back to the (z,t) coordinates [7], we get

$$A_z^p(z,t) = \frac{1}{4}\iint_{(z,t)} \varepsilon \frac{\partial E^{inc}(z',t')}{\partial t'}\frac{\partial(\xi',\eta')}{\partial(z',t')}\, dt'dz', \tag{10}$$

where the Jacobian is given by

$$\frac{\partial(\xi',\eta')}{\partial(z',t')} = \begin{vmatrix} 1 & -1 \\ c & c \end{vmatrix} = 2c \quad .$$

The limit of integration in Eq. (10) should now be changed to (z,t), which is illustrated in Fig. 2. The upper limits in Eq. (9) give

$$\xi' = \xi \text{ and } \eta' = \eta,$$

which in the (z,t) coordinates become

$$ct' + z' = ct + z \text{ and } ct' - z' = ct - z.$$

If we integrate t' first in Eq. (10) the two limits are given by the straight lines

$$t' = t + \frac{(z-z')}{c} \text{ and } t' = t - \frac{(z-z')}{c} .$$

The integration in Eq. (10) now becomes

$$A_z^p(z,t) = \frac{\varepsilon c}{2} \int_{-\infty}^{z} \int_{-\infty}^{t' - \frac{(z-z')}{c}} \frac{\partial E^{inc}(z',t')}{\partial t'} dt'$$

$$+ \frac{\varepsilon c}{2} \int_{z}^{\infty} \int_{-\infty}^{t' + \frac{(z-z')}{c}} \frac{\partial E^{inc}(z',t')}{\partial t'} dt'$$

$$= \frac{\varepsilon c}{2} \int_{-\infty}^{z} E^{inc}(z', t - \frac{(z-z')}{c}) dt' + \frac{\varepsilon c}{2} \int_{z}^{\infty} E^{inc}(z', t$$

$$+ \frac{(z-z')}{c}) dt' = \frac{\varepsilon c}{2} \int_{-\infty}^{\infty} E^{inc}(z', t - \frac{|z-z'|}{c}) dt'. \quad (11)$$

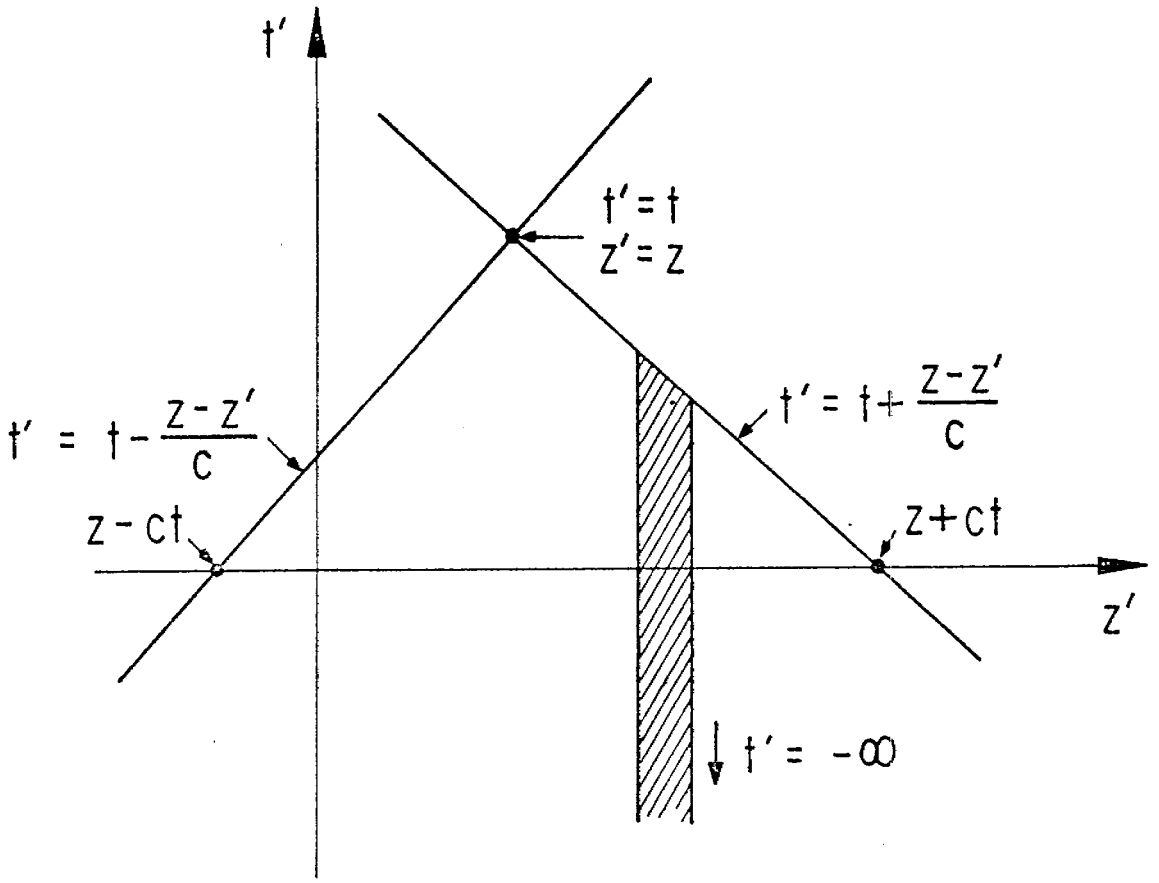

Fig. 2 The limits of integration for A_z^P in (z',t') space

Since the differential equation, Eq. (6), is only limited to the surface of the antenna, we have

$$A_z^p(z,t) = \frac{1}{2Z_0} \int_0^L E^{inc}(z', t - \frac{|z-z'|}{c})dt', \tag{12}$$

where L is the total length of the wire, and $Z_0 = \frac{1}{\varepsilon c}$ the intrinsic impedance of the medium.

Combining the straight wire version of Eqs. (4) and (12), and the homogeneous solutions to the wave equation, Eq. (6), the integral equation is thus established as follow,

$$\iint_S \frac{J_z(z', t - \frac{|\vec{r}-\vec{r}'|}{c})}{4\pi|\vec{r} - \vec{r}'|} ds' = \frac{1}{2Z_0} \int_0^L E^{inc}(z', t - \frac{|z-z'|}{c})dz'$$

$$+ f_1(ct-z) + f_2(ct+z), \tag{13}$$

where $J_z(\vec{r},t)$ is the current density along the wire, $f_1(ct-z)$ and $f_2(ct+z)$ are the homogeneous solutions determined by the boundary conditions that $J_z(0,t) = J_z(L,t) = 0$.

As $\vec{r}$ and $\vec{r}'$ represent any two points on the surface of the wire, we have

$$|\vec{r}-\vec{r}'| = [(z-z')^2 + 4a^2 \sin^2 \frac{|\phi-\phi'|}{2}]^{1/2}, \tag{14}$$

where ϕ and ϕ' are the circumferential angles of the observation

point and the source point in the cylindrical coordinates. Due to the axial symmetry of the wire, Eq. (14) needs to be satisfied only for one value of ϕ. We select $\phi = 0$, yielding

$$|\vec{r}-\vec{r}'| = [(z-z')^2 + 4a^2 \sin^2 \frac{\phi'}{2}]^{1/2} . \qquad (15)$$

For a thin wire, we can neglect the transverse current. This implies that the time delay term in $J_z(z',t')$ can be approximated by $|z-z'|/c$. For this axially symmetric current density, the current is given by

$$I(z,t) = 2\pi a \, J_z(z,t) , \qquad (16)$$

where a is the radius of the wire. Eq. (13) can now be expressed in the following form,

$$\int_0^L \int_{-\pi}^{\pi} \frac{I(z', t - \frac{|z-z'|}{c})}{8\pi^2 \sqrt{(z-z')^2 + 4a^2 \sin^2 \frac{\phi'}{2}}} d\phi' \, dz'$$

$$= \frac{1}{2Z_0} \int_0^L E^{inc}(z', t - \frac{|z-z'|}{c}) dz'$$

$$+ f_1(ct-z) + f_2(ct+z) . \qquad (17)$$

When the observation and source points are far apart, it is possible to use the thin wire approximation for the kernel in Eq. (13), and we obtain,

$$\int_0^L \frac{I(z',t-\frac{|z-z'|}{c})}{4\pi\sqrt{(z-z')^2+a^2}}\,dz' = \frac{1}{2Z_0}\int_0^L E^{inc}(z',t-\frac{|z-z'|}{c})\,dz'$$

$$+ f_1(ct-z) + f_2(ct+z). \qquad (18)$$

Either Eq. (17) or (18) can be used for the solution of the thin wire problems by means of numerical techniques on a digital computer. When the observation point is close to the source point, the thin wire approximation is not very accurate and the singularity has to be treated with care. The physical interpretation of either Eq. (17) or (18) helps directly towards the procedures of numerical solutions and will be discussed more fully in the following section.

III. THE NUMERICAL METHOD AND RESULTS FOR A SINGLE ANTENNA OR SCATTERER

In the first part of this section, we present the physical interpretation and the numerical method in solving Eq. (17) or Eq. (18). Since the method of numerical approximation of integrals etc. is well documented [8], we shall present only a brief outline. The novelty of the method perhaps lies in the use of the concept of characteristic curves. This method has been proved to be elegant and efficient for this type of problems [9]. In the second part, some results of the computation are presented.

3.1 The Numerical Method

(a) The physical interpretation and the sampling scheme.

Equation (17) or its thin wire version, Eq. (18), indicates that for a specific pair of values (z,t_0), the current $I(z',t_0 - \frac{|z-z'|}{c})$ lies on the straight lines $t - \frac{z-z'}{c} = t_0$ and $t + \frac{z-z'}{c} = t_0$ in (z',t) plane as shown in Fig. 3. For a discrete set of parameter t_0, these straight lines form two families of trajectories, α and β, known as the characteristic curves [9]. On the α-family of curves, $t_0 = t + \frac{z-z'}{c}$, or

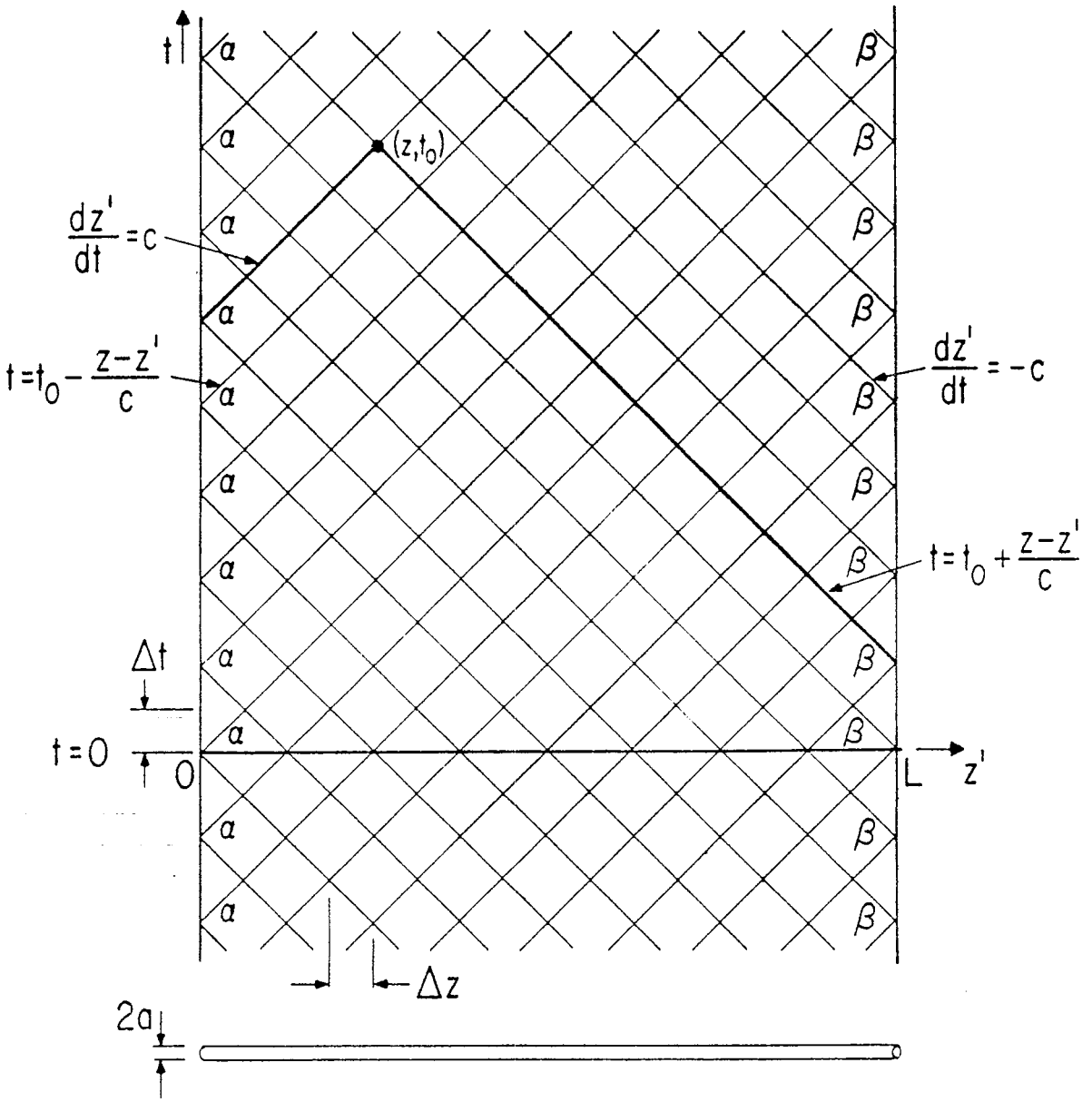

Fig. 3 z'-t' diagram showing the two families of α and β characteristic curves. $\Delta z = L/16$.

$$\frac{dz'}{dt} = c, \tag{19}$$

we find current waves propagating along the wire in the + z direction. Similarly on the β-family of curves we find current waves in the - z direction, as

$$\frac{dz'}{dt} = - c. \tag{20}$$

For efficient numerical procedures, the wire is discretized into N+1 points, where N is an even integer. As observed from Fig. 3, at the time t = 0, N = 8. The distance between two neighboring grid points is

$$2\Delta z = L/N. \tag{21}$$

The time step, as demanded to be consistent with Eqs. (19) and (20), is

$$\Delta t = \Delta z/c. \tag{22}$$

From Fig. 3, it is observed that the next time line, t = Δt, has only N sampling points and does not include the two end points of the wire. These two sampling arrangements, of t = 0 and t = Δt, alternate, and are necessary for this type of sampling scheme involving characteristic curves.

The solution of the homogeneous wave equation $f_1(ct-z)$ is invariant along an α-curve, which is characterized by a constant value of ct-z. Similarly $f_2(ct+z)$ is invariant along a β-curve. These

two functions should be included in the equations to account for the multiple reflection of the current at the two ends of the wire. Mathematically, the homogeneous solutions enforce the boundary conditions $I(0,t) = I(L,t) = 0$. In effect they summarize the history of current by the boundary conditions so that the integration may terminate at $z' = 0$ and $z' = L$.

(b) The numerical approximation of the current integral.

The simplest numerical approximation of the current integral, i.e. the integral on the left hand side of either equation, is perhaps the point testing or the pulse testing method [8]; both of these were used by Sayre [3]. In the present work, to achieve better accuracy, the current is interpolated. As observed from Eq. (17) or Eq. (18), the current, propagating in the directions of the characteristic curves, should have smooth values along them; hence the interpolation is carried out linearly along the characteristic curves.

Consider a point (z',t') between the two grid points $(z-(k+1)\Delta z,\ t-(k+1)\Delta t)$ and $(z-k\Delta z,\ t-k\Delta t)$, such that all these three points lie on the α characteristic curve through the observation point (z,t). The current $I(z',t')$, using linear interpolation, is given by

$$I(z',t') = I_k + \frac{z'-z+k\Delta z}{\Delta z}\,(I_k - I_{k+1}), \tag{23}$$

where I_k stands for the current $I(z-k\Delta z,\ t-k\Delta t)$.

In Eq. (17), the current integral between the two grid points

is thus,

$$\text{Current Integral}\Big|_{-(k+1)}^{-k} = \int_{z-(k+1)\Delta z}^{z-k\Delta z} \int_{-\pi}^{\pi} \frac{I_k\left[1 + \frac{z'-z+k\Delta z}{\Delta z}\right] - I_{k+1}\left[\frac{z'-z+k\Delta z}{\Delta z}\right]}{8\pi^2 \sqrt{(z-z')^2 + 4a^2 \sin^2 \frac{\phi'}{2}}} d\phi' dz'$$

Let $z'' = z'-z$, then,

$$\text{Current Integral}\Big|_{-(k+1)}^{-k} = \int_{-(k+1)\Delta z}^{-k\Delta z} \int_{-\pi}^{\pi} \frac{I_k\left[1 + \frac{z''+k\Delta z}{\Delta z}\right] - I_{k+1}\left[\frac{z''+k\Delta z}{\Delta z}\right]}{8\pi^2 \sqrt{z''^2 + 4a^2 \sin^2 \frac{\phi'}{2}}} d\phi' dz'' = T_1^k I_k + T_2^k I_{k+1}, \qquad (24)$$

where, for $k \neq 0$

$$T_1^k = \frac{1}{8\pi^2}\left[(k+1)S_1^k + S_2^k\right],$$

$$T_2^k = -\frac{1}{8\pi^2}\left[kS_1^k + S_2^k\right], \qquad (25)$$

and,

$$S_1^k = 2 \int_{-(k+1)\Delta z}^{-k\Delta z} \int_0^{\pi} \frac{1}{\sqrt{z''^2 + 4a^2 \sin^2 \frac{\phi'}{2}}} d\phi' dz'' ,$$

$$S_2^k = \frac{2}{\Delta z} \int_{-(k+1)\Delta z}^{-k\Delta z} \int_0^{\pi} \frac{z''}{\sqrt{z''^2 + 4a^2 \sin^2 \frac{\phi'}{2}}} d\phi' dz'' . \qquad (26)$$

The two integrals of Eq. (26) are evaluated numerically using Simpson's rule.

In Eq. (18); the current integral with the thin wire approximation between the two grid points is,

$$\text{Current Integral} \Big|_{-(k+1)}^{-k} = \int_{z-(k+1)\Delta z}^{z-k\Delta z} \frac{I_k[1 + \frac{z'-z+k\Delta z}{\Delta z}] - I_{k+1}[\frac{z'-z+k\Delta z}{\Delta z}]}{4\pi \sqrt{(z-z')^2 + a^2}} dz' = T_1^k I_k + T_2^k I_{k+1} , \qquad (27)$$

where, for $k \neq 0$

$$T_1^k = \frac{1}{4\pi} [(k+1)S_1^k + S_2^k],$$

$$T_2^k = -\frac{1}{4\pi} [kS_1^k + S_2^k], \qquad (28)$$

and,

$$S_1^k = \ell n \left[\frac{-k\Delta z + \sqrt{(k\Delta z)^2 + a^2}}{-(k+1)\Delta z + \sqrt{(k+1)^2\Delta z^2 + a^2}} \right]$$

$$S_2^k = \frac{1}{\Delta z} \left[\sqrt{(k\Delta z)^2 + a^2} - \sqrt{(k+1)^2\Delta z^2 + a^2} \right] . \qquad (29)$$

In Table I, the T_1^k and T_2^k values obtained from Eq. (25) and Eq. (28) are compared for three different values of Δz for $\Omega = 2 \log (L/a) = 10$. It is observed that in general the two sets of values agree very well, except near the singular point $z' = z$. This implies that the simpler Eq. (18) is a good approximation of Eq. (17).

At the singular point $z' = z$ and $\phi' = 0$ the singularity is integrable. We shall perform the integration by means of the method of auxiliary integral [10]. In this method, the integrand is separated into two parts, one is analytically integrable which takes care of the integrable singularity, and the other contains no singularity at all. For this singularity, we have to evaluate Eq. (25) and Eq. (26) with $k = 0$. Applying the method of auxilary integral to S_1^0, we have,

$$S_1^0 = 2 \int_{-\Delta z}^{0} \int_{0}^{\pi} \frac{\cos \frac{\phi'}{2}}{\sqrt{z''^2 + 4a^2 \sin^2 \frac{\phi'}{2}}} d\phi' dz''$$

$$+ 2 \int_{-\Delta z}^{0} \int_{0}^{\pi} \frac{1 - \cos \frac{\phi'}{2}}{\sqrt{z''^2 + 4a^2 \sin^2 \frac{\phi'}{2}}} d\phi' dz''$$

	Thin Wire		Exact	
k	T_1^k	T_2^k	T_1^k	T_2^k
0	0.16330	0.06957	←	
1	0.03063	0.02436	0.03053	0.02430
2	0.01720	0.01503	0.01718	0.01502
3	0.01199	0.01089	0.01198	0.01089
4	0.00921	0.00855	0.00920	0.00854
5	0.00747	0.00703	0.00747	0.00703

(a) $\Omega = 10$, $\Delta z = 1/16 = 0.0625$

k	Thin Wire		Exact	
	T_1^k	T_2^k	T_1^k	T_2^k
0	0.11770	0.06131	←	
1	0.03029	0.02419	0.02989	0.02397
2	0.01714	0.01500	0.01707	0.01494
3	0.01197	0.01088	0.01194	0.01086
4	0.00920	0.00854	0.00919	0.00853
5	0.00747	0.00703	0.00746	0.00702

(b) $\Omega = 10$, $\Delta z = \frac{1}{32} = 0.03125$

k	Thin Wire		Exact	
	T_1^k	T_2^k	T_1^k	T_2^k
0	0.07924	0.04908	←	
1	0.02905	0.00076	0.02784	0.00076
2	0.01692	0.00075	0.01665	0.00075
3	0.01189	0.00073	0.01180	0.00073
4	0.00916	0.00072	0.009118	0.00072
5	0.00745	0.00071	0.00743	0.00071

(c) $\Omega = 10$, $\Delta z = \frac{1}{64} = 0.015625$

TABLE I: Values of T_1^k, T_2^k

$$= 4 \left[\frac{\Delta z}{2a} \sinh^{-1} \frac{2a}{\Delta z} + \sinh^{-1} \frac{\Delta z}{2a} \right]$$

$$+ 4 \int_0^{\pi/2} \ell n \left[\frac{\Delta z}{2a \sin\theta} + \sqrt{1 + \left(\frac{\Delta z}{2a \sin\theta} \right)^2} \right] (1-\cos\theta) d\theta, \qquad (30)$$

and,

$$S_2^0 = \frac{2}{\Delta z} \int_{-\Delta z}^{0} \int_0^{\pi} \frac{z'' \cos \frac{\phi'}{2}}{\sqrt{z''^2 + 4a^2 \sin^2 \frac{\phi'}{2}}} d\phi' dz''$$

$$+ \frac{2}{\Delta z} \int_{-\Delta z}^{0} \int_0^{\pi} \frac{z''(1 - \cos \frac{\phi'}{2})}{\sqrt{z''^2 + 4a^2 \sin^2 \frac{\phi'}{2}}} d\phi' dz''$$

$$= - \frac{1}{\Delta z} \left[2 \sqrt{4a^2 + \Delta z^2} + \frac{\Delta z^2}{a} \ell n \left(\frac{2a}{\Delta z} + \sqrt{1 + \frac{4a^2}{\Delta z^2}} \right) - 4a \right]$$

$$- 4 \int_0^{\pi/2} \left[\sqrt{\Delta z^2 + 4a^2 \sin^2\theta} - 2a \sin\theta \right] (1-\cos\theta) d\theta. \qquad (31)$$

The integrals in Eq. (30) and Eq.(31) are evaluated by the Simpson's rule method. In Table I, a few values of T_1^0 and T_2^0 are included.

Consider the case that the source point (z',t') is between the two grid points (z+kΔz, t-kΔt) and (z+(k+1)Δz, t-(k+1)Δt), all are located to the right of the observation point (z,t) and lie on the same β characteristic curve. The current I(z',t'), using linear interpolation, is

The total current integral in Eq. (17) or Eq. (18), integrated from $z' = 0$ to $z' = L$, is thus approximated by

$$\text{Current Integral} = \sum_{k=0}^{k=\frac{z}{\Delta z}} [T_1^k I_k + T_2^k I_{k+1}]$$

$$+ \sum_{k=0}^{k=\frac{L-z}{\Delta z}} [T_1^k I'_k + T_2^k I'_{k+1}] \ . \qquad (34)$$

(c) The numerical approximation of the electric field integral.

The incident electric field integral is less important than the current integral since the latter contains the unknown quantity. The former integral is thus evaluated by means of the trapezoidal rule of numerical integration, yielding at the observation point (z,t) the following approximation,

$$\text{E Integral} = \frac{\Delta z}{2} \left[\sum_{k=0}^{k=\frac{z}{\Delta z}} (E_k + E_{k+1}) + \sum_{k=0}^{k=\frac{L-z}{\Delta z}} (E'_k + E'_{k+1}) \right], \qquad (35)$$

where E_k stands for $E^{inc}(z-k\Delta z,\ t-k\Delta t)$, and E'_k for $E^{inc}(z+k\Delta z,\ t-k\Delta t)$.

(d) The evaluation of the unknown current and f_1, f_2.

Eq. (17) or Eq. (18) can be approximated, numerically, using Eq. (34) and Eq. (35), by the following equation

$$2T_1^0 I_0 + T_2^0(I_1+I_1') + \sum_{k=1}^{k=\frac{z}{\Delta z}} [T_1^k I_k + T_2^k I_{k+1}]$$

$$+ \sum_{k=1}^{k=\frac{L-z}{\Delta z}} [T_1^k I_k' + T_2^k I_{k+1}'] = \frac{\Delta z}{4Z_0} \left[\sum_{k=0}^{k=\frac{z}{\Delta z}} (E_k+E_{k+1}) \right.$$

$$\left. + \sum_{k=0}^{k=\frac{L-z}{\Delta z}} (E_k' + E_{k+1}') \right] + f_1(ct-z) + f_2(ct+z). \qquad (36)$$

The current at time t may be found from Eq. (36) if the current and f_1, f_2 along the α and β characteristics are known prior to time t. To facilitate the determination of the functions f_1 and f_2, we extend the characteristics beyond the t = 0 line as shown in Fig. 3. Realizing that $f_1(ct-z) = f_2(ct+z) = 0$ for $t \leq 0$, and that f_1 and f_2 are invariant along these characteristics, we find that these functions vanish as long as the (z,t) pair is on a characteristic curve which extends into the region $t \leq 0$. To find the current at $t = \Delta t$, we shall first assume the wire to be unexcited, i.e., $I(z,0) \equiv 0$, and by the previous reasoning, we find $f_1(\Delta t \mp z) = 0$. Thus, the current at $t = \Delta t$ is readily found from Eq. (36). At $t = 2\Delta t$, since $I(0,t) = I(L,t) = 0$ we find $f_1(2c\Delta t)$ and $f_2(2c\Delta t+L)$ on the outgoing characteristics at z = 0 and z = L respectively. Using similar steps, we may find I(z,t) at $t = 2\Delta t$, $3\Delta t$, $4\Delta t$, $\cdots$, and $f_1(ct)$ and $f_2(ct+L)$ at $t = 4\Delta t$, $6\Delta t$, $\ldots$. The computation is a step-by-step time-marching process, based on the condition that the currents prior to the point under evaluation are known. Hence, if we can

perform the calculation for one time line, we are able to compute the current for all subsequent time.

From Fig. 3, we observe that if the wire is sampled at N+1 points, then, for one transit time,

$$\tau = L/c, \tag{37}$$

which is the time for the current to travel between the two ends of the wire, we have 2N+1 time steps. Therefore, there are $(N+\frac{1}{2}) \times (2N+1)$ sampling points within one transit time. At each point, one has to use 2N+1 values to compute the current and electric field integrals. The total number of operation is thus proportional to N^3.

In most cases computed, N is chosen to be 8 and the results are quite finely resolved.

3.2 Results.

The correctness and accuracy of the results may be checked by converting the time domain data into the frequency domain. In Fig. 4, we present the input admittance of a center-fed dipole with $\Omega = 10$ as a function of frequency. The agreement with Harrington's frequency domain result [8] is good. The input admittance is given by the quotient of the Fourier transform of the transient input current to the Fourier transform of the driving voltage.

For the case of a scatterer with an incident electric field $E_0(t')$, propagating at an angle ϕ to the z axis as shown in Fig. 1(b), the effective incident electric field at a point z on the scatterer, after taking the incident angle and delay into account, is

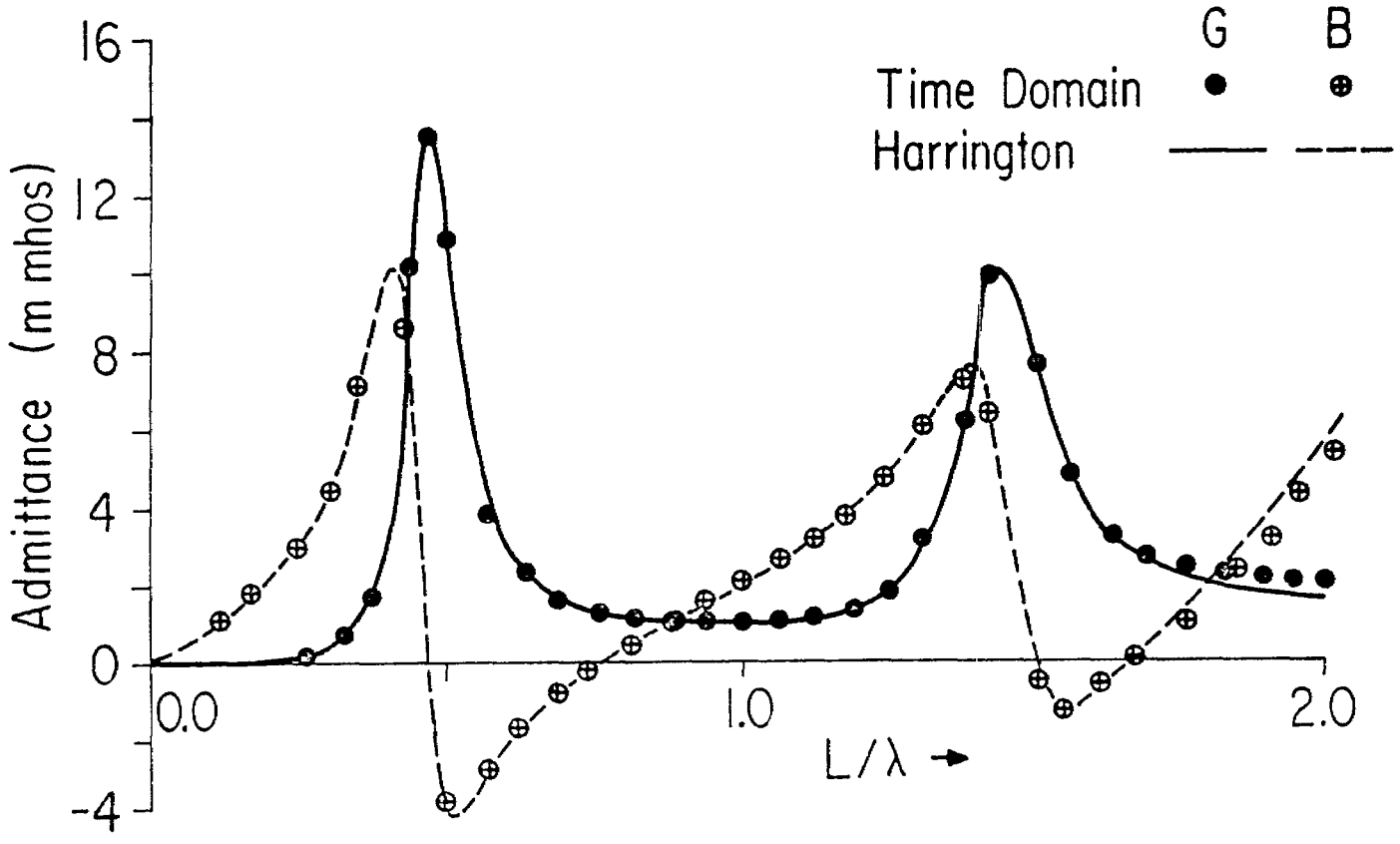

Fig. 4 Input-admittance of a center-fed dipole with $\Omega = 10$.

$$E^{inc}(z',t') = E_0(t' - \frac{z'}{c}\cos\phi)\sin\phi \quad \text{for } t' \geq \frac{z'}{c}\cos\phi$$

$$= 0 \qquad \text{for } t' < \frac{z'}{c}\cos\phi \ . \tag{38}$$

Here, we have taken the time origin of $E_0(t')$ to be at the point $z' = 0$ on the scatterer. The trajectory of this wave propagation can be represented in the (z',t') diagram. In Fig. 5, the wavefronts of propagation for a few incident angles are shown in the (z',t') diagram together with the characteristic grids. It is observed that except for $\phi = 0°$ (end incident) and $\phi = 90°$ (broadside incident), the wavefront trajectory intersects the characteristic curves at points other than the grid points. Physically, the wavefront of the incident field propagates faster along the wire than the induced current, hence, the initial induced current at each point on the wire is the same and is readily evaluated by means of Eq. (36). We thus know that at each point the wavefront intersects with a characteristic curve, current is induced and this value and the electric field quantity have to be taken into account in the subsequent computation. This process of evaluation is described more fully in the Appendix.

In Fig. 6, the center currents of a scatterer with $\Omega = 2\ln(L/a) = 10$ under a unit step incident electric field are presented for the cases $\phi = 30°$, $60°$ and $90°$. There appears to be a gradual transition from sharp to smooth responses as the electric field becomes more broadsided.

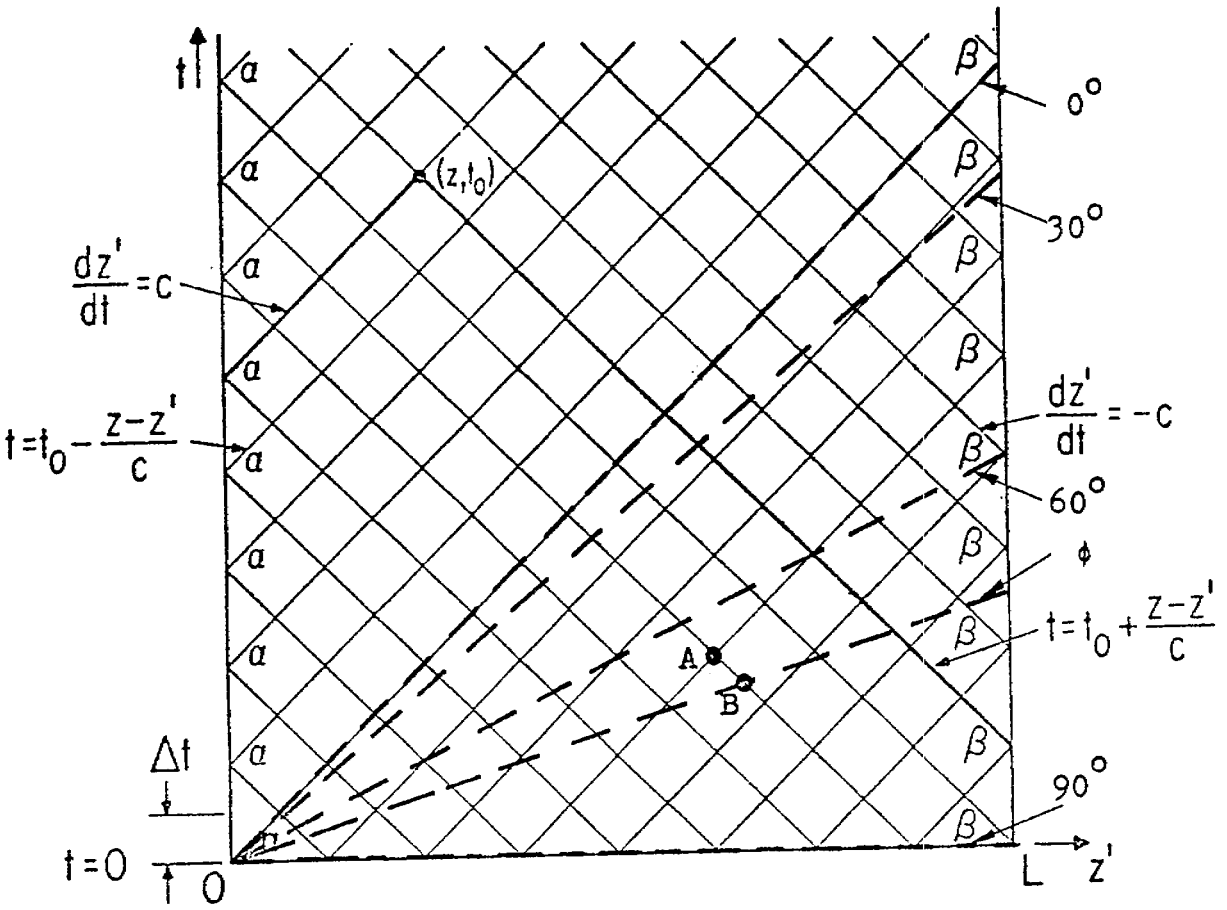

Fig. 5 z'-t' diagram showing the intersections of the wavefronts of E^{inc} at various incident angles with the characteristics curves.

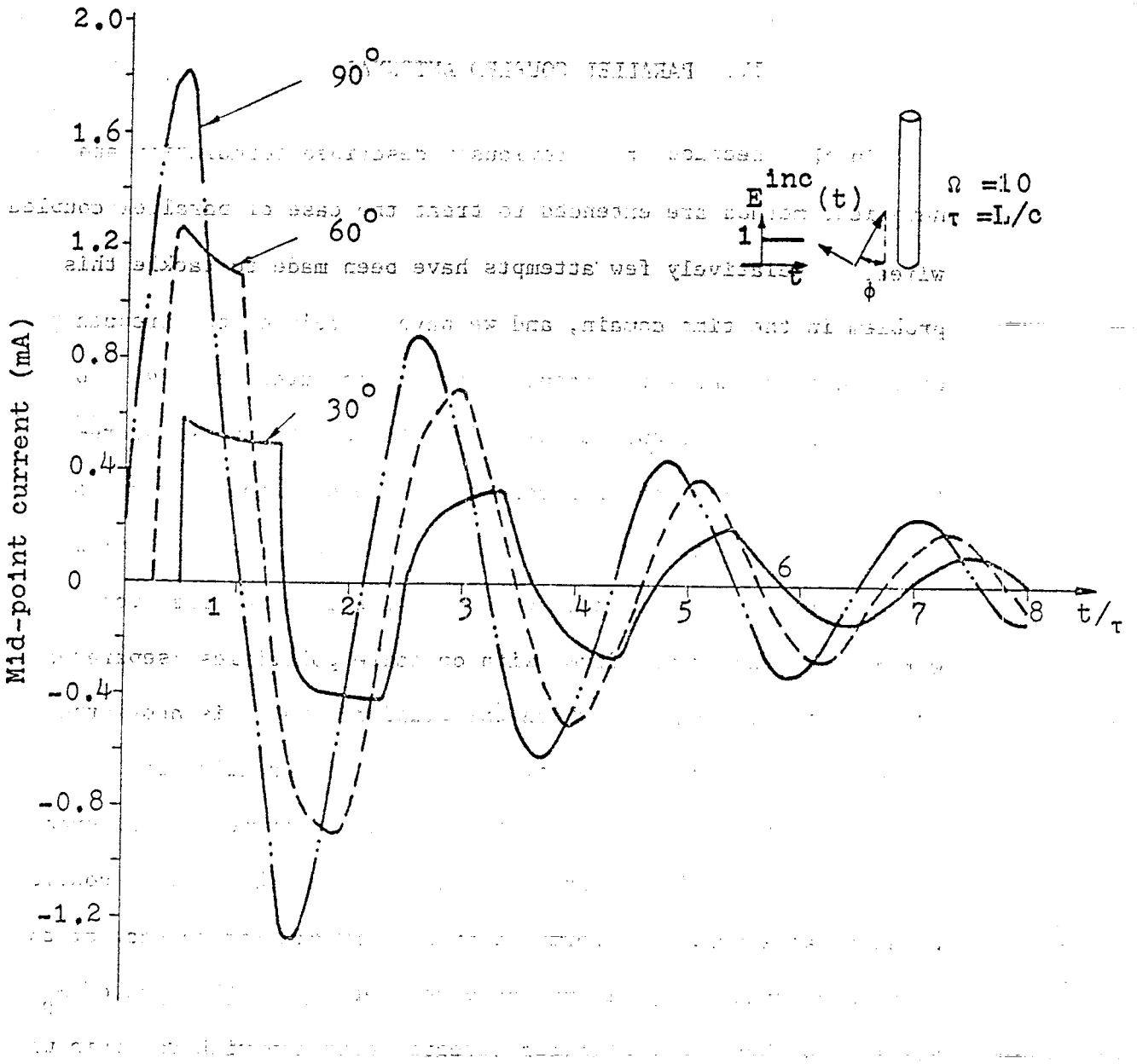

Fig. 6 Mid-point current responses of a scatterer under a unit-step electric field excitation incident at angles ϕ = 30°, 60° and 90°.

IV. PARALLEL COUPLED ANTENNAS

In this section, the previously described formulation and numerical method are extended to treat the case of parallel coupled wires. Relatively few attempts have been made to tackle this problem in the time domain, and we have to rely on the frequency domain data to check the accuracy of the computed results. Abo-Zena and Beam [11], and Tesche [12] obtained the transient responses of a wire above a conducting ground plane by means of the Fourier transform of the computed frequency domain results. By the image theory, this case is equivalent to two identical wires, driven by waveforms with opposite polarities, separated by twice the distance by which the original wire is above the ground plane. The method they employed is inherently slow.

By adding the effect of mutual coupling between the antennas, Eq. (17) or Eq. (18) can easily be extended to the case of coupled parallel antennas. The formulation is very similar to that of the frequency domain and will not be given here. For the case of N_p wires, we have the following integral equation with the thin wire approximation,

$$\int_{L_j} \frac{I_j(z',t - \frac{|z-z'|}{c})}{4\pi\sqrt{(z-z')^2 + a_j^2}}\,dz' + \sum_{\substack{i=1\\ i\neq j}}^{N_p} \int_{L_i} \frac{I_i(z',t - \frac{1}{c}\sqrt{(z-z')^2 + b_{ij}^2})}{4\pi\sqrt{(z-z')^2 + b_{ij}^2}}\,dz'$$

$$= \frac{1}{2Z_0} \int_{L_j} E^{inc}(z',t - \frac{|z-z'|}{c})dz' + f_{1j}(ct-z) + f_{2j}(ct+z)$$

$$j = 1, \ldots, N_p, \qquad (39)$$

where the subscript j denotes the wire on which z is located, b_{ij} is the perpendicular separation between wires i and j, and a_j is the radius of wire j.

Equation (39) is similar to Eq. (18) except for the integrals under the summation sign which account for the coupling effect of the neighboring wires. The numerical solution procedure follows closely to that of a single wire. At time t and at each point z on wire j, there is only one unknown, i.e. $I_j(z,t)$, since the extra integrals contain quantities that are time-retarded due to the separation between the wires i and j, and are known for this step-by-step time-marching process.

Since the mutual coupling effect is of secondary importance, to save the computational effort, the integrals under the summation sign in Eq. (39) need not be evaluated as accurately as the first integral. Consequently, the trapezoidal rule of numerical integration is used. The values b_{ij} are in general large when compared with (z-z'), there are no singularity problems for these mutual

coupling terms. However, the time delay, being $\frac{1}{c}\sqrt{(z-z')^2 + b_{ij}^2}$, may not be a multiple of the time step Δt, hence the current value $I_i(z', t - \frac{1}{c}\sqrt{(z-z')^2 + b_{ij}^2})$ may not be that of a grid point. This current value, being at an intermediate point between two grid points at the same z' value, is obtained by a simple time-wise interpolation of the current values at these two grid points. Although interpolation along characteristic curves offers higher accuracy, the simple method mentioned above is adequate for its purpose and has a considerably greater advantage of saving in computational effort.

To compare with the frequency domain results [22]-[24], a pair of non-staggered, identical parallel wires is chosen.

The frequency domain results by performing Fourier transforms on the transient results agree very well with known data. In Fig. 7, we present the transient responses of the mid-point currents of two identical wires with $\Omega = 10$, separated by half the wire length. In Fig. 7(a), wire 1 is center-fed with a unit step while wire 2 is not directly driven. We observe the general increase in current magnitude of wire 1 compared with that of an isolated wire. In Fig. 7(b), the wires are driven by unit step voltages with opposite polarities. There is an enhancement of the current magnitude.

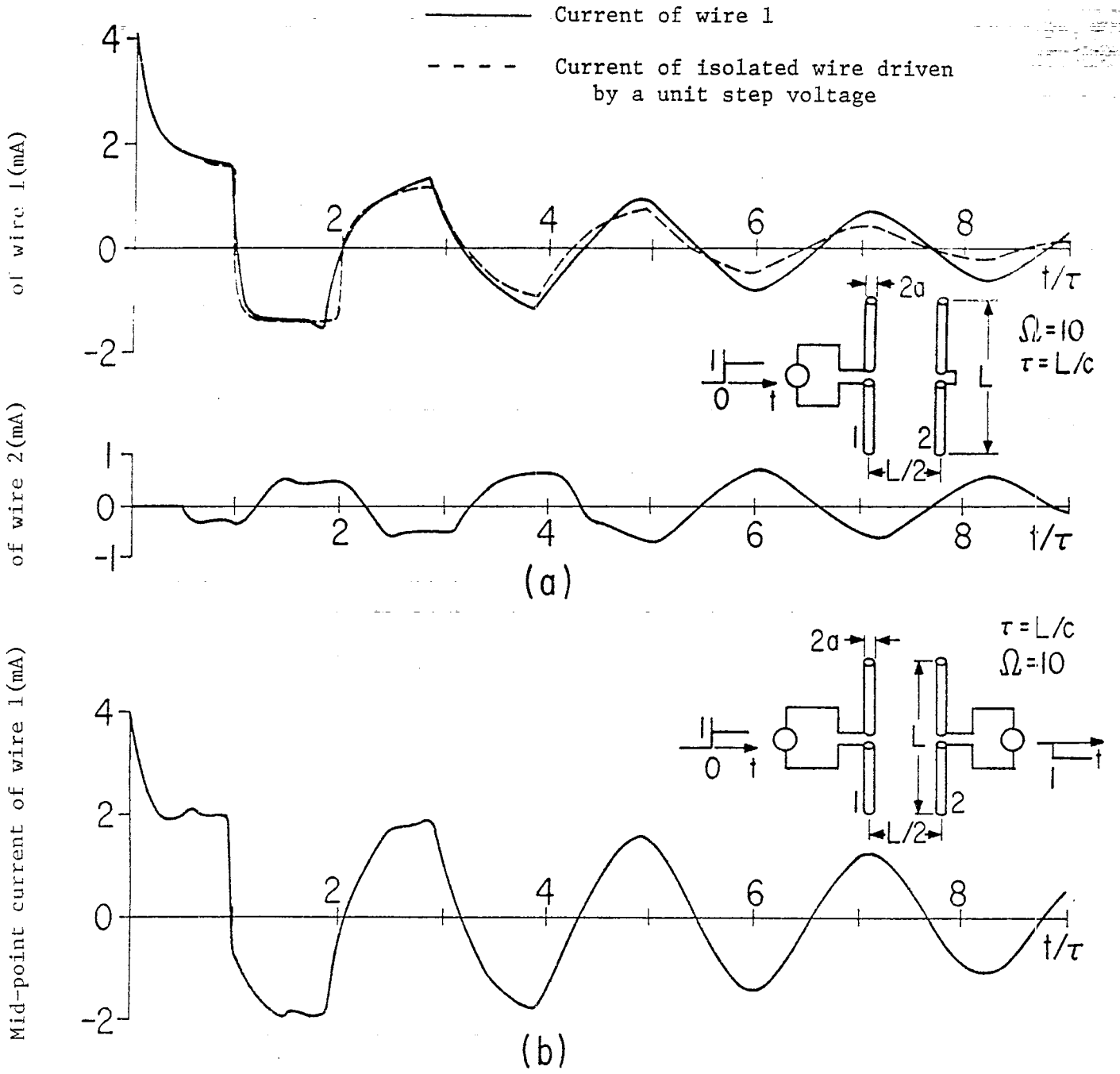

Fig. 7 Mid-point current responses of a pair of non-staggered identical coupled parallel wires separated by half the wire length, with $\Omega = 10$.

(a) Only one wire is driven by a unit step, and

(b) the two wires are driven by two unit step voltages with opposite polarities.

V. LOADED WIRES AND LOSSY WIRES

The effect of a source resistance on an antenna is important to understand a practical radiation system. It also turns out that the solution of this problem in the time domain is useful for studying the transient response of an antenna driven via a transmission line; this latter problem will be presented in the next section. When the scatterer is loaded with some lumped elements across a certain length, or if the wire itself is not perfectly conducting, Eq. (17) and Eq. (18) have to be slightly modified. The study of this problem is essential to the understanding of a practical receiving system.

5.1 Antennas Driven With a Source Resistance.

Consider an antenna driven at a position $z = z_0$ by a voltage source $v_s(t)$ with a source resistance R_s, as shown in Fig. 8. The actual voltage across the excitation gap which is assumed to be within one cell length is

$$v(t) = v_s(t) - I(z_0,t)R_s \ . \tag{40}$$

For an observation point (z,t), the electric field integral contains only terms across the gap at $z = z_0$, and is equal to the voltage across the gap with a suitable time delay. Hence,

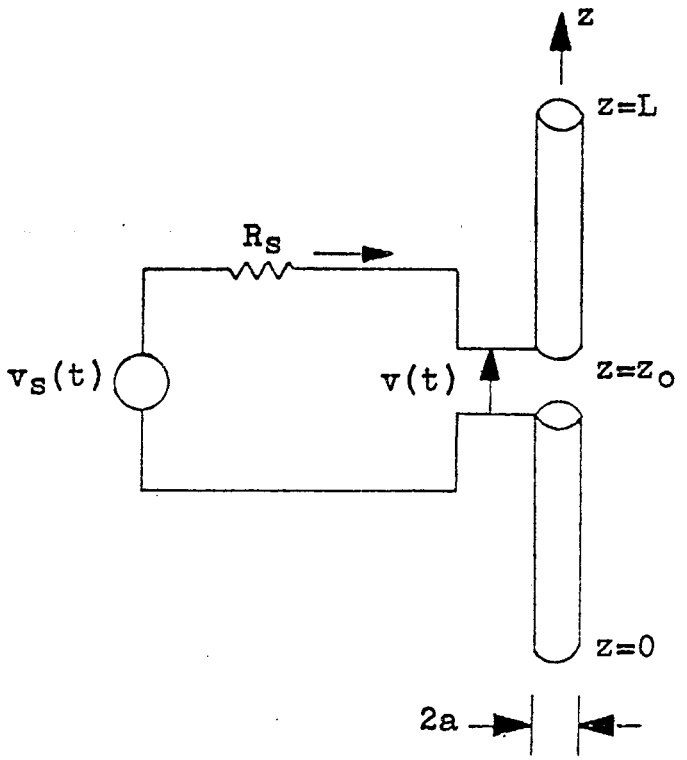

Fig. 8 Antenna driven by a voltage source with a source resistance.

$$\text{E Integral} = v(t - \frac{|z-z_0|}{c})$$

$$= v_s(t - \frac{|z-z_0|}{c}) - I(z_0, t - \frac{|z-z_0|}{c})R_s. \qquad (41)$$

Using Eq. (41) instead of Eq. (35), we obtain the following equation,

$$2T_1^0 I_0 + T_2^0(I_1+I_1') + \sum_{k=1}^{k=\frac{z}{\Delta z}} [T_1^k I_k + T_2^k I_{k+1}]$$

$$+ \sum_{k=1}^{k=\frac{L-z}{\Delta z}} [T_1^k I_k' + T_2^k I_{k+1}']$$

$$= \frac{1}{2Z_0}[v_s(t - \frac{|z-z_0|}{c}) - I(z_0, t - \frac{|z-z_0|}{c})R_s]$$

$$+ f_1(ct-z) + f_2(ct+z) \ . \qquad (42)$$

For $z \neq z_0$, the above equation is readily solved for the unknown $I_0 = I(z,t)$. For $z = z_0$, the current on the right hand side of (42) is not known, and the evaluation of I_0 is slightly different to the former case. It is interesting to note that if $\frac{R_s}{2Z_0} << 2T_1^0$, the source resistance has very little effect on the behavior of the antenna; if $\frac{R_s}{2Z_0} >> 2T_1^0$, it would result in a very small current.

5.2 Wires With Distributed Loss.

For the case that the wire has a distributed resistance $\rho(z)$ Ω/meter, Eq. (17) and Eq. (18) have to be modified to take this loss into account.

On the surface of the wire, the total electric field is given by

$$E(z,t) = E^{inc}(z,t) + E^{s}_{z}(z,t) = I(z,t)\rho(z), \qquad (43)$$

From Eq. (5), we have

$$\frac{\partial^2 A_z(z,t)}{\partial z^2} - \frac{1}{c^2}\frac{\partial^2 A_z(z,t)}{\partial t^2} = -\varepsilon \frac{\partial}{\partial t}\left[E^{inc}(z,t) - I(z,t)\rho(z)\right]. \qquad (44)$$

Carrying out similar derivation as from Eq. (7) to (13), we find that there is one extra current term appearing in the current integral, and the new equation with the thin wire approximation is,

$$\int_0^L \left[\frac{1}{4\pi\sqrt{(z-z')^2 + a^2}} + \frac{1}{2Z_0}\rho(z')\right] I(z', t - \frac{|z-z'|}{c})dz'$$

$$= \frac{1}{2Z_0}\int_0^L E^{inc}(z', t - \frac{|z-z'|}{c})dz' + f_1(ct-z) + f_2(ct+z). \qquad (45)$$

Thus, the effect of the distributed resistance is to modify the kernel of the current integral. Eq. (45) is readily solved by similar numerical method as outlined in Section III.

In Fig. 9 , the center-point current for a scatterer with $\Omega = 10$ is presented for constant distributed resistances $\rho(z) = 10^{-6}$ and 10^{-8} Ω/meter under a unit step electric field incident at 30° to the z axis.

5.3 Scatterers With Lumped Loads.

Eq. (45) can be easily modified to treat the case of lumped loads on a scatterer. For a single load at $z = z_0$, located within one cell length, the electric field across the load is

$$E(z,t) = \frac{1}{\Delta z} v_L(t)\delta(z-z_0), \tag{45}$$

where $\delta(z-z_0)$ is the δ function, $v_L(t)$ is the voltage drop across the load and is given by

$$v_L(t) = I(z_0,t)R_L \qquad \text{for a resistance } R_L,$$

$$v_L(t) = L_L \frac{dI(z_0,t)}{dt} \qquad \text{for an inductance } L_L,$$

and

$$v_L(t) = \frac{1}{C_L} \int_0^t I(z_0,t)dt \quad \text{for a capacitance } C_L.$$

For more complicated loading, $v_L(t)$ is in more involved form and network analysis techniques have to be applied. Substituting Eq.

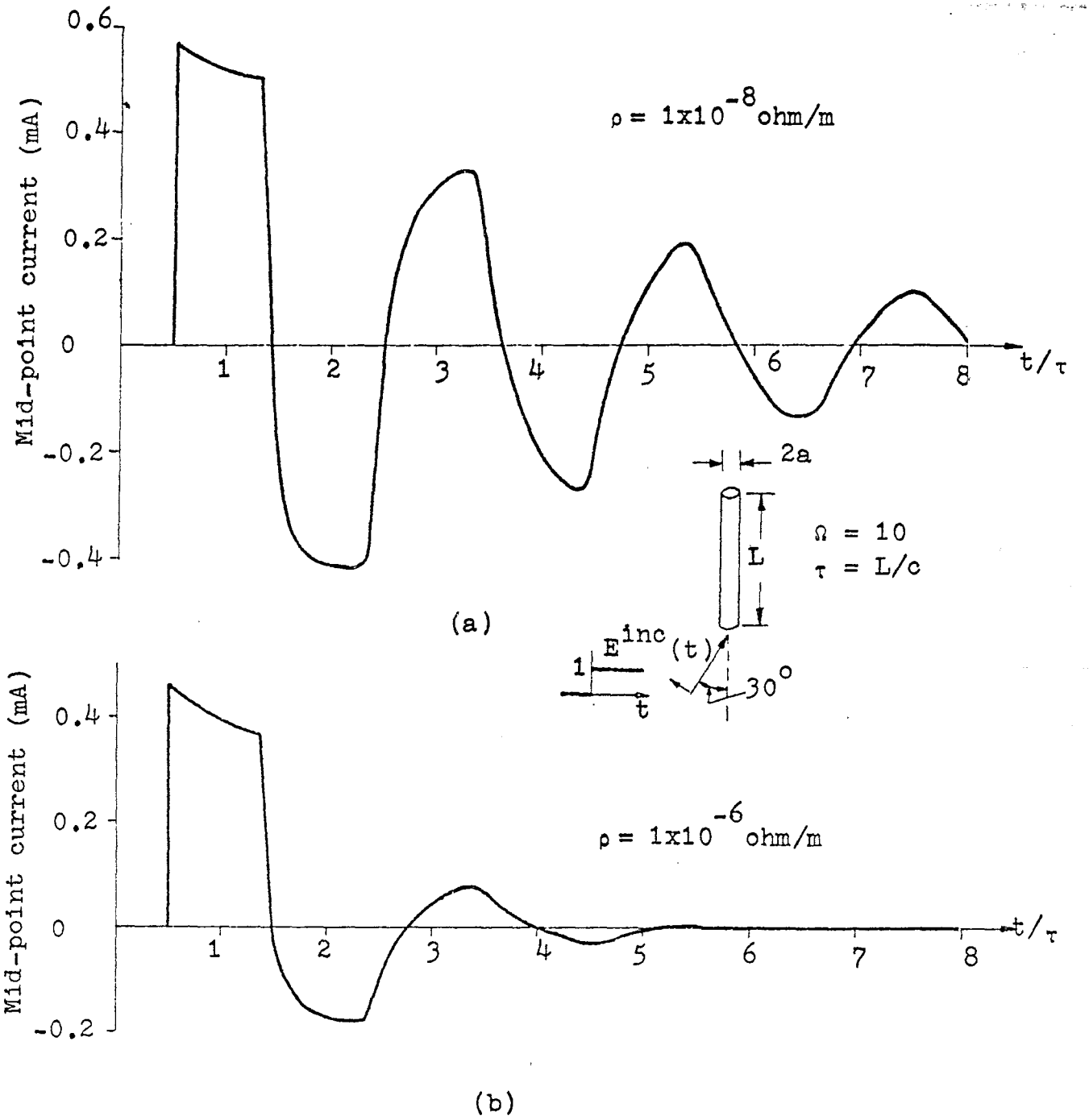

Fig. 9 Mid-point current responses of a lossy scatterer under a unit step electric field excitation incident at 30°. $\Omega = 10$.

(a) Resistance per unit length = 10^{-8} Ω/m and

(b) 10^{-6} Ω/m.

(46) into Eq. (45), we have

$$\int_0^L \frac{I(z',t-\frac{|z-z'|}{c})}{4\pi\sqrt{(z-z')^2+a^2}}\,dz' = \frac{1}{2Z_0}\Big[\int_0^L E^{inc}(z',t-\frac{|z-z'|}{c})dz' - v_L(t-\frac{|z-z_0|}{c})\Big] + f_1(ct-z) + f_2(ct+z). \qquad (47)$$

The time derivative or integration that may appear in $v_L(t)$ are numerically approximated. For $z \neq z_0$, Eq. (47) is readily evaluated by the previously described procedures. For $z = z_0$, the unknown current appears also on the right hand side of the equation and has to be combined together with the unknown current on the left hand side of Eq. (47).

In Fig. 10, the load currents for a center-loaded scatterer under the excitation of a 30° incident plane wave are presented. The resistive load reduces the current amplitude of the unloaded-wire. The inductive load increases the time between two subsequent zero crossings of the current, indicating an effective lengthening of the wire; the waveform is also smoothed out. The capacitive load shows the opposite effect and effectively shortens the wire; the waveform is sharpened up.

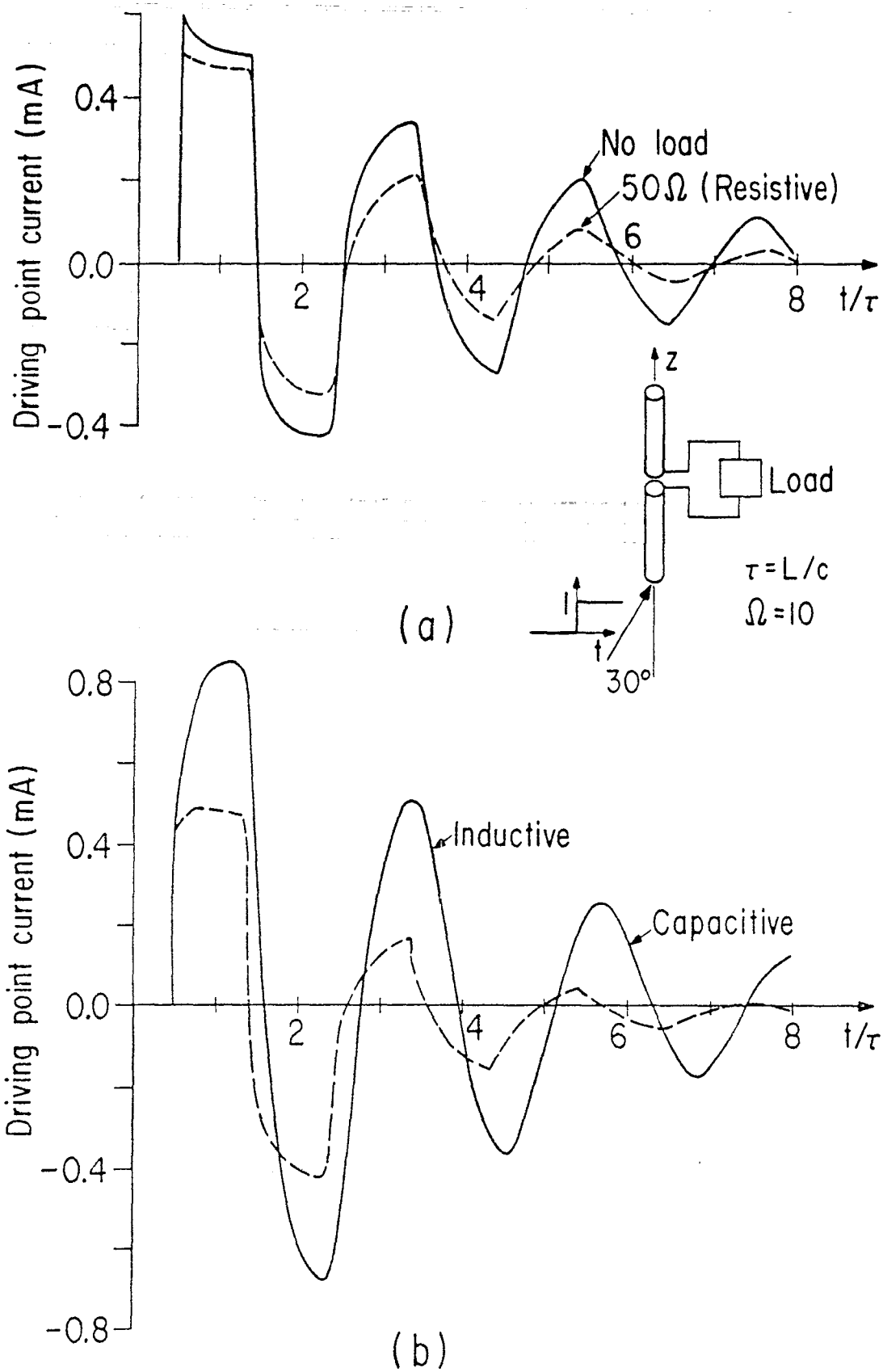

Fig. 10 Induced load current responses on a center-loaded scatterer under the excitation of a 30° incident unit step electric field.

(a) No load and 50 Ω resistive load, and (b) Inductive Load of j 63 Ω at full wave frequency, and capacitive load of -j 53 Ω at full wave frequency.

VI. CONCLUSIONS

The formulation and numerical solution of the time-space integral equation is useful in the understanding of the transient behavior of linear antennas and scatterers. This is of particular interest to the performance of RES.

This approach has been applied to a wide range of linear thin-wire problems, including arrays and wires with losses.

APPENDIX

INTERSECTION OF THE WAVEFRONT AND THE CHARACTERISTIC CURVES

The wavefront is taken to begin at $z' = 0$ at time $t = 0$. It intersects with the characteristic curves only between $t = 0$ and $t = \tau$, as shown in Fig. 5.

(a) α characteristic curves.

The α characteristic curves are defined by,

$$z' = ct + z_\alpha, \tag{A1}$$

where z_α is the intersection of the characteristic curves with the z' axis. The wavefront front is expressed as

$$z' = ct/\cos\phi \ . \tag{A2}$$

The intersection point is thus

$$ct = \frac{\cos\phi}{1-\cos\phi} z_\alpha \tag{A3}$$

and

$$z' = \frac{1}{1-\cos\phi} z_\alpha \ . \tag{A4}$$

If $z' > L$, then, there is no intersection along the length of the wire.

(b) β characteristic curves.

The β characteristic curves are defined by,

$$z' = - ct + z_\beta \ , \tag{A5}$$

where z_β is the intersection of the characteristic curve with the z' axis. Together with Eq. (A2) , we have

$$ct = \frac{\cos\phi}{1 + \cos\phi} z_\beta \ , \tag{A6}$$

and

$$z' = \frac{1}{1 + \cos\phi} z_\beta . \tag{A7}$$

If $z' > L$, then, there is no intersection along the length of the wire.

(c) The current integral.

If the intersection point with a β characteristic curve is B with $z' = z_B$, and the next nearest grid point along this characteristic curve is A, as shown in Fig. 5, the current integral has to be evaluated slightly differently to what previously described because $z_{AB} = z_B - z_A$ is not, in general, a multiple of Δz. For $z - z_A = k\Delta z$, we have, for the Eq. (17) version,

$$\text{Current Integral} \Big|_{-z_B}^{-k} = \int_{-(z-z_B)}^{-k\Delta z} \int_{-\pi}^{\pi}$$

$$\frac{I_k\left[1 + \frac{z''+k\Delta z}{z_{AB}}\right] - I_B\left[\frac{z''+k\Delta z}{z_{AB}}\right]}{8\pi^2\sqrt{z''^2 + 4a^2\sin^2\frac{\phi'}{2}}}\, dz''d\phi' \qquad \text{(A8)}$$

This integral is similar to that of Eq. (24) and can be evaluated by similar techniques. The thin wire version, Eq. (18), follows the similar pattern with z_{AB} replacing Δz as in Eq. (A8). If the current at point A is unknown, i.e. $z = z_A$, then, Eqs. (30) and (31) are applicable with again z_{AB} replacing Δz.

For the intersection with α characteristic curves, similar expressions are obtained as above.

(d) The electric field integral.

For the same configuration as in Fig. 5, the electric field integral from point B to point A, using the trapezoidal rule is

$$\text{E Integral}\Big|_{-z_B}^{-k} = \frac{1}{2z_{AB}}\left[E^{inc}(z_B,\ t_B) + E^{inc}(z_A,\ t_A)\right] \qquad \text{(A9)}$$

REFERENCES

[1] See, for example, Wu, T. T., "Transient response of a dipole antenna," J. Math. Phys., 2, pp. 892-894, Nov.-Dec. 1961.

[2] Tesche, F. M., "On the behavior of thin-wire scatterers and antennas arbitrarily located within a parallel plate region," Sensor and Simulation Notes 135, August 1971.

[3] Sayre, E. P., "Transient response of wire antennas and scatterers," Tech. Rept. TR-69-4, Syracuse University, Syracuse, New York, May 1969.

[4] Bennett, C. L. and Martine, J., "A space-time integral equation solution for currents on wire structures with arbitrary excitation," URSI Fall Meeting, Columbus, Ohio, 1970.

[5] Miller, E. K., Burke, G. J., and Poggio, A. J., "Time domain analysis of wire antennas," URSI Fall Meeting, Los Angeles, California, 1971.

[6] Bennett, C. L., and Weeks, W. L., "Transient scattering from conducting cylinders," IEEE Trans. on Antennas and Propagation, AP-18, pp. 627-633, September 1970.

[7] Kaplan, W., Advanced Calculus, Mass., Addison-Wesley, 1952.

[8] Harrington, R. F., Field Computation by Moment Methods, New York, MacMillan, 1968.

[9] Courant, R., and Hilbert, D., Method of Mathematical Physics, Vol. II, New York, Interscience, 1962.

[10] Lin, S. H., and Mei, K. K., "Numerical solution of dipole radiation in a compressible plasma," IEEE Trans. on Antennas and Propagation, AP-16, pp. 235-241, March 1968.

[11] Abo-Zena, A. M., and Beam, R. E., "Transient radiation field of a pulse-excited linear antenna parallel to a conducting plane," IEEE 1970 G-AP International Symposium Digest, pp. 310-317, September 1970.

[12] Tesche, F. M., "Numerical analysis of an arbitrarily located antenna within a parallel plate region," IEEE 1971 G-AP International Symposium Digest, September 1970.